



---

## Figures and figure supplements

Genome mining unearths a hybrid nonribosomal peptide synthetase-like-pteridine synthase biosynthetic gene cluster

**Hyun Bong Park *et al***

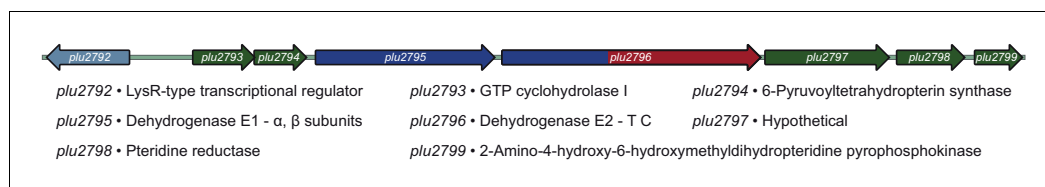


**Figure 1.** The peptidine biosynthetic locus. Green, pteridine synthesis genes; Blue, pyruvate dehydrogenase-like genes; Red, NRPS-like genes. T, thiolation domain; C, condensation domain.

DOI: [10.7554/eLife.25229.003](https://doi.org/10.7554/eLife.25229.003)

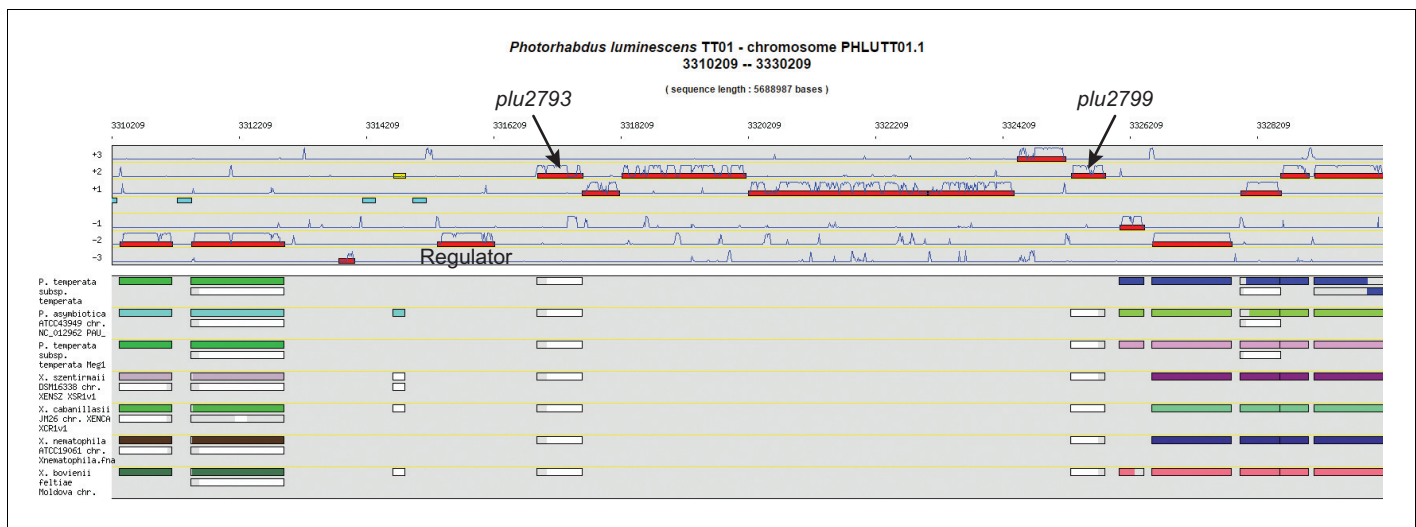


**Figure 1—figure supplement 1.** Genome synteny analysis using MicroScope. Genome synteny analysis revealed a genomic island in *P. luminescens* TT01 (note absence of biosynthetic genes in phylogenetically related species, lower panel) harboring a number of enzymes possessing homology to pteridine and NRPS biosynthetic machineries (+1, +2, and +3 reading frames, upper panel). The regulator in the genomic island was not included in our design, as the pathway was placed under the control of a T7 promoter.

DOI: 10.7554/eLife.25229.004

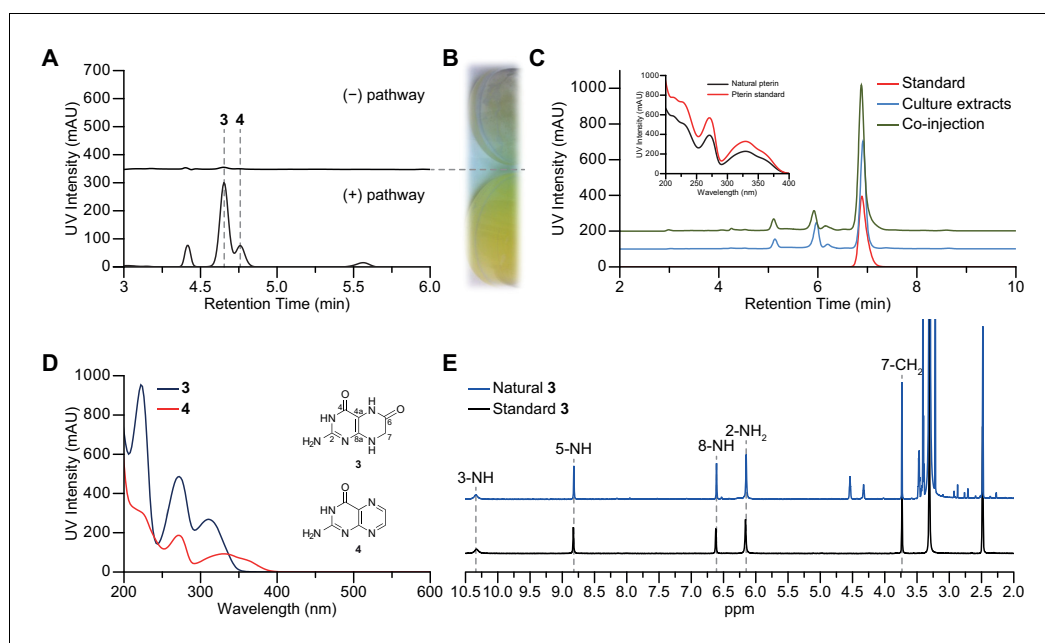


**Figure 2.** Production of 7,8-dihydroxanthopterin (3) and pterin (4) by heterologous expression. (A) HPLC traces (310 nm) of butanol extracts showing compounds 3 and 4 being over-produced in the heterologous expression strain. (B) The edge of a culture flask growing *E. coli* BAP1 carrying an empty vector pET28a (top), and a culture flask growing *E. coli* BAP1 carrying the wild-type peptidine pathway (bottom). (C) HPLC traces (310 nm) from HPLC co-injection with authentic pterin (4), and UV absorption spectral comparison between natural and authentic pterin (inset). (D) UV-vis absorption spectra of compounds 3 and 4. (E)  $^1\text{H}$  NMR comparison of natural (blue) and standard (black) 3 in  $\text{DMSO}-d_6$ .

DOI: [10.7554/eLife.25229.005](https://doi.org/10.7554/eLife.25229.005)

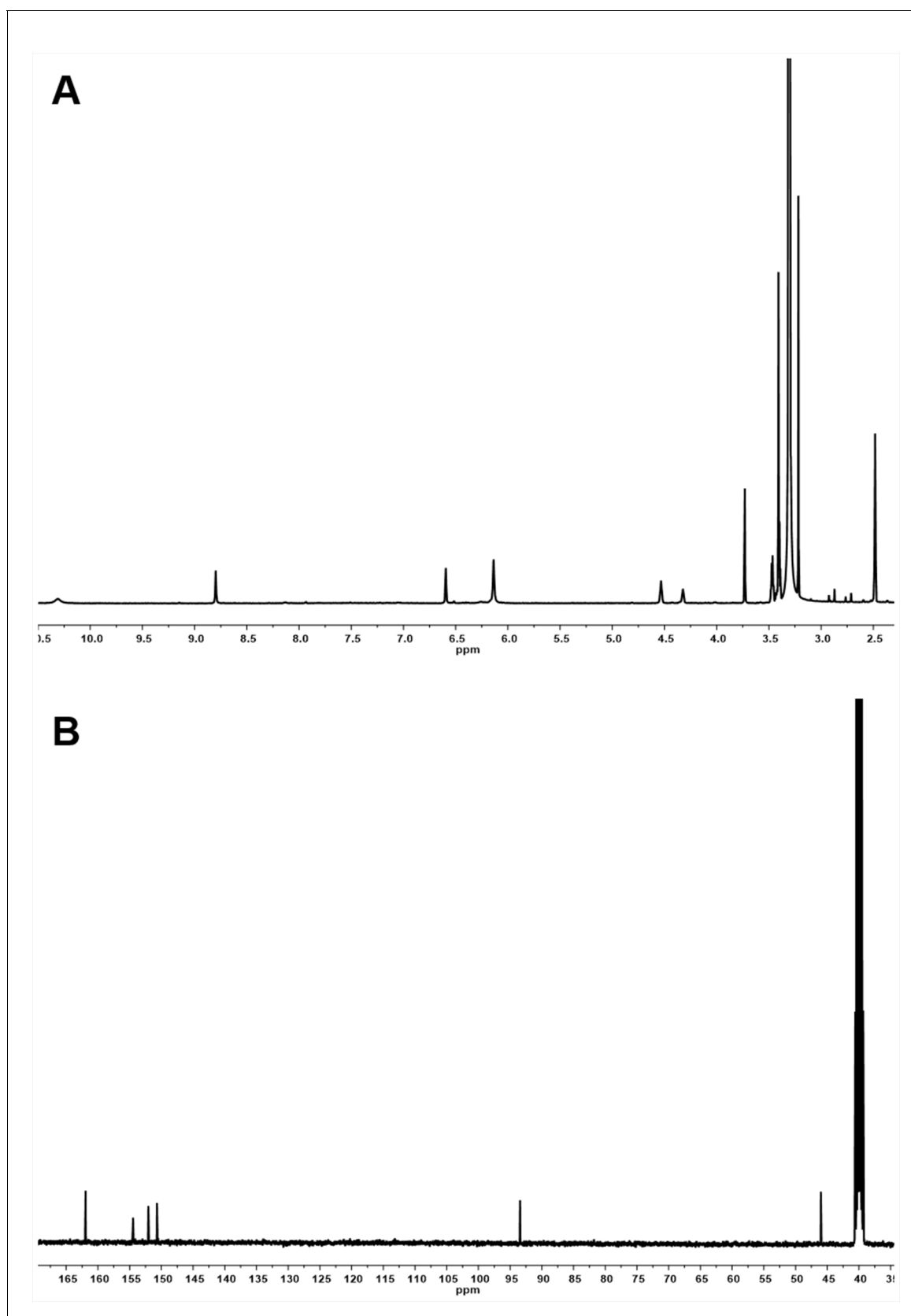


**Figure 2—figure supplement 1.**  $^1\text{H}$  and  $^{13}\text{C}$  NMR spectra of compound 3. (A)  $^1\text{H}$  NMR spectrum of compound 3 in DMSO- $d_6$ . (B)  $^{13}\text{C}$  NMR spectrum of compound 3 in DMSO- $d_6$ .

Figure 2—figure supplement 1 continued on next page

Figure 2—figure supplement 1 continued

DOI: [10.7554/eLife.25229.006](https://doi.org/10.7554/eLife.25229.006)

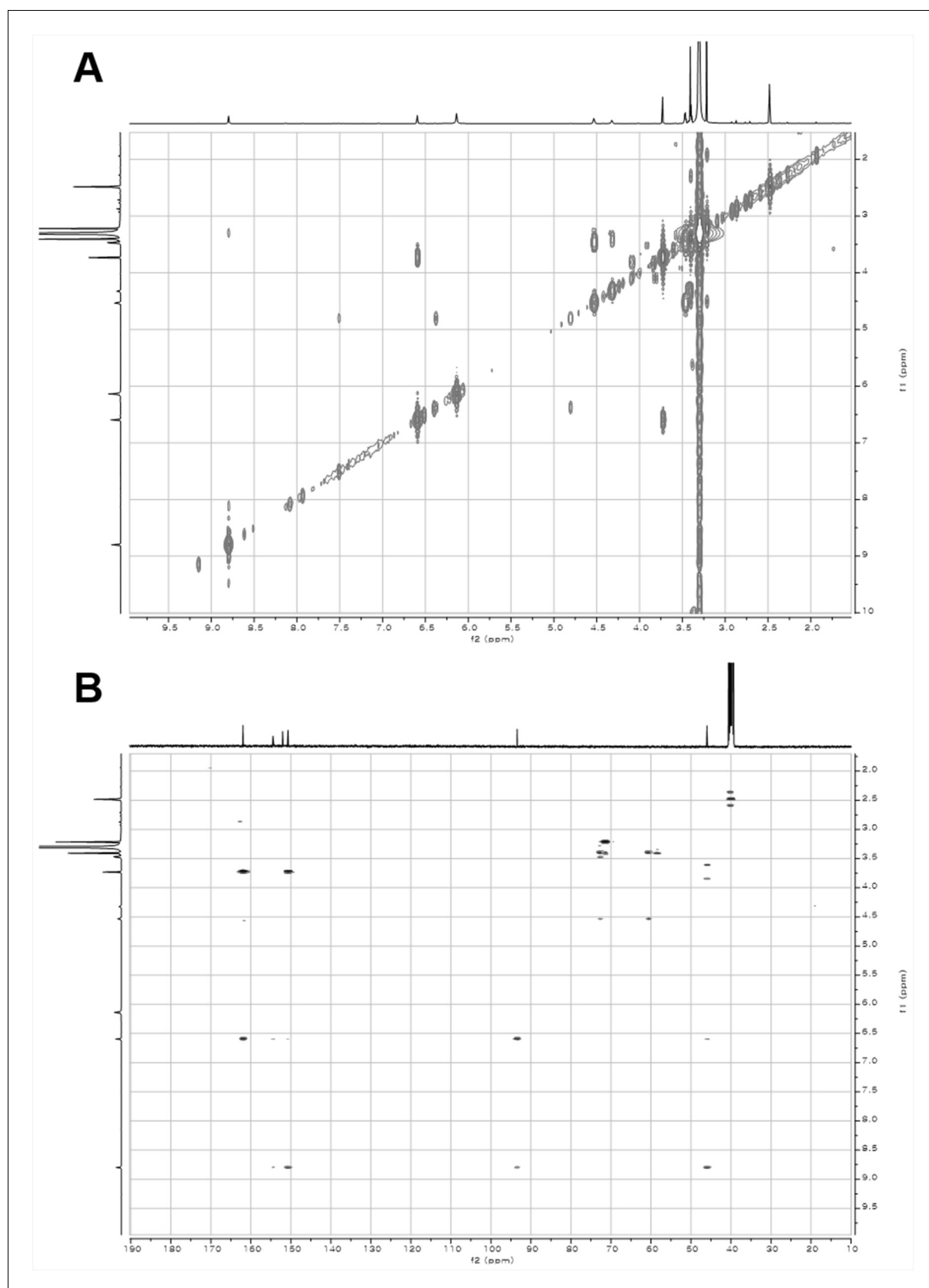


**Figure 2—figure supplement 2.** 2D- (gCOSY and gHMBCAD) NMR spectra of compound **3**. (A) gCOSY NMR spectrum of compound **3** in DMSO- $d_6$ . (B) gHMBCAD NMR spectrum of compound **3** in DMSO- $d_6$ .

DOI: [10.7554/eLife.25229.007](https://doi.org/10.7554/eLife.25229.007)



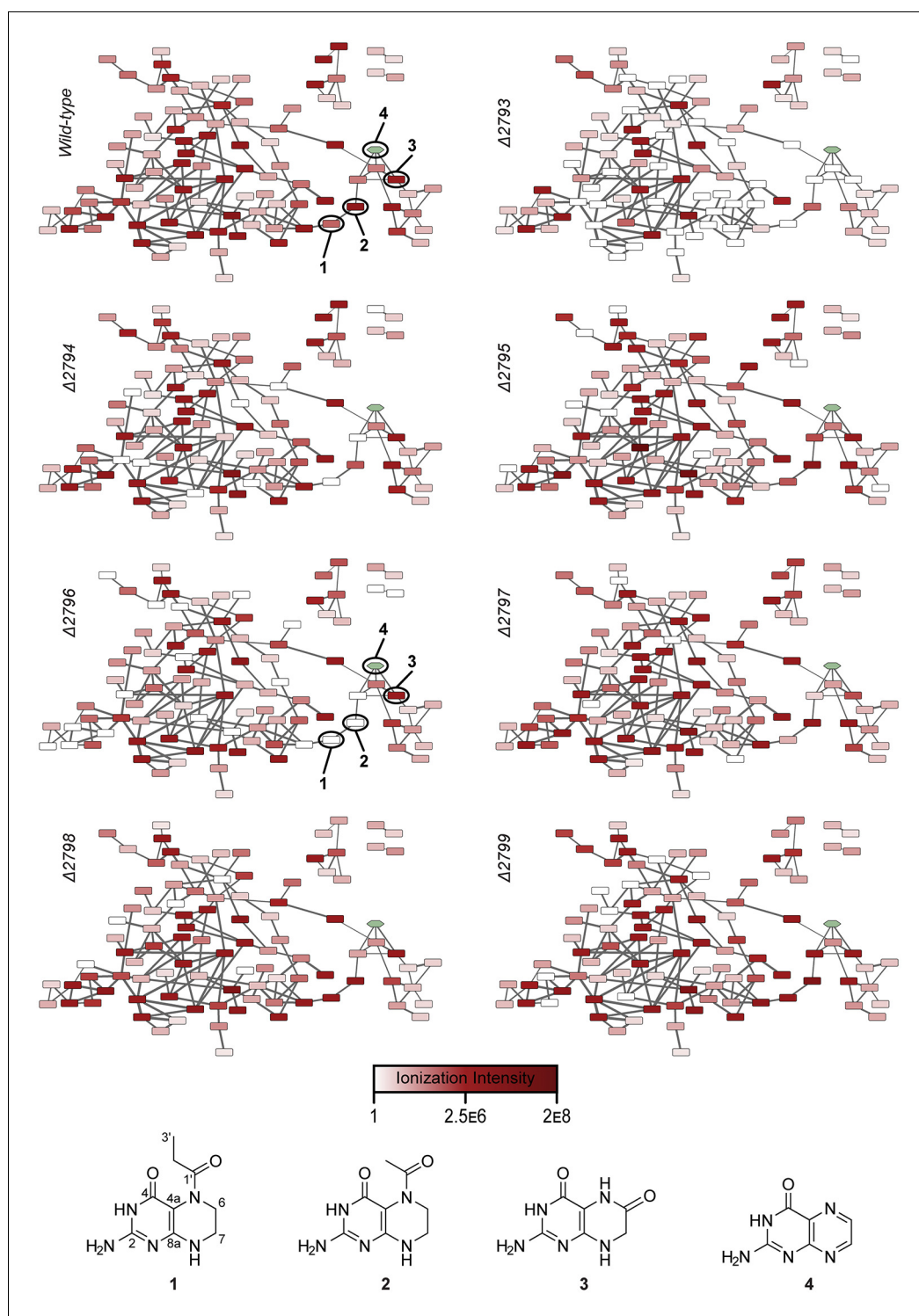


**Figure 3.** Relative abundances of wild-type pathway-dependent metabolites in wild-type and mutant peptididine pathways. The average ionization intensity is depicted for each molecular feature under a given genetic condition (wild-type and  $\Delta plu2793$  through  $\Delta plu2799$ ). Alterations in abundance are correlated with changes in nodal color intensity among genetic constructs, allowing visual assessment of product distributions for a given mutation. See **Figure 3—figure supplement 2** for information on mass of pathway-dependent metabolites. Structural characterization of compounds 1 and 2 is shown in **Figure 3—figure supplements 4–10**, **Table 2**, and the Materials and methods section.

DOI: [10.7554/eLife.25229.009](https://doi.org/10.7554/eLife.25229.009)

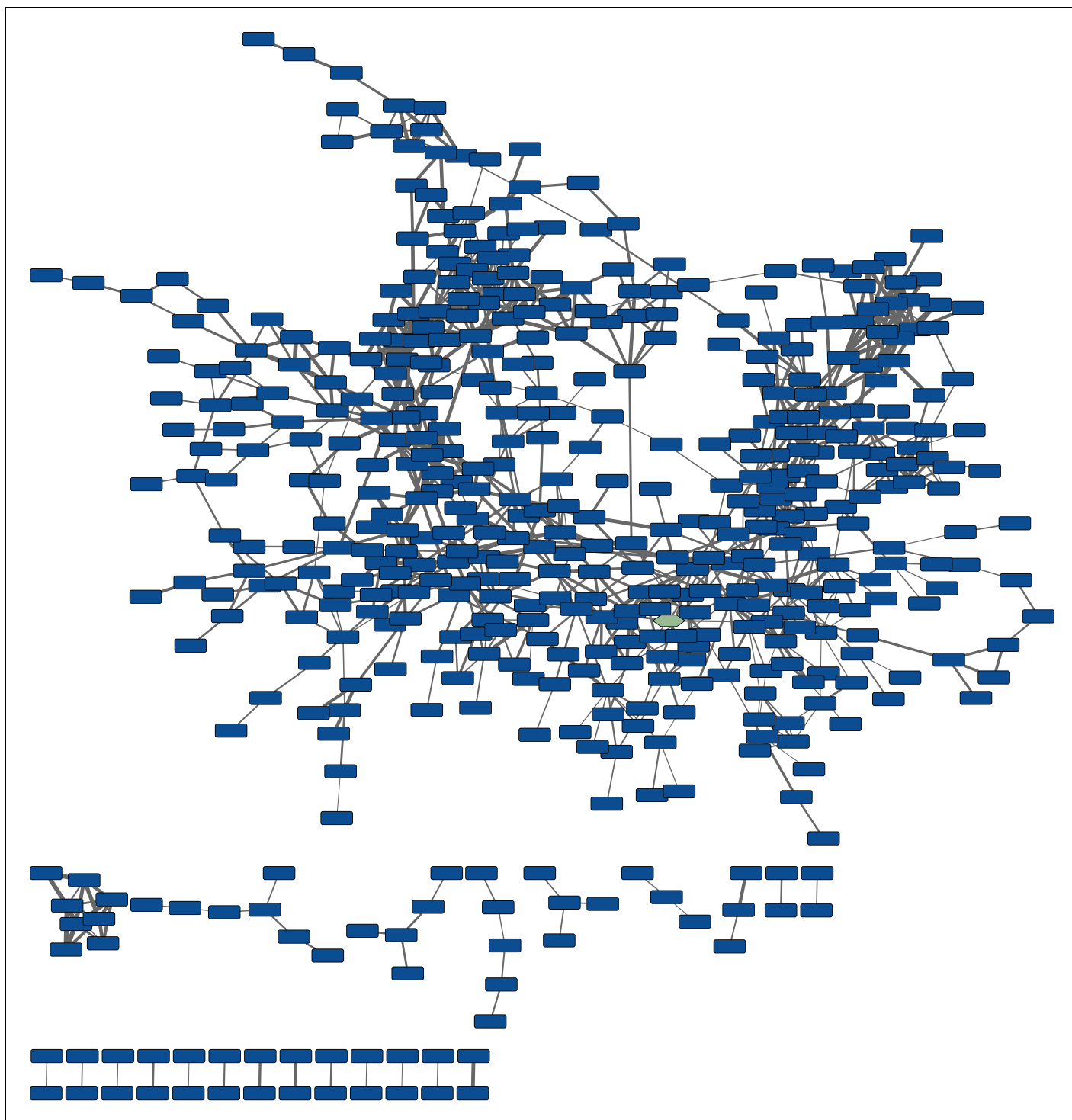


**Figure 3—figure supplement 1.** Untargeted molecular networking of culture extracts from cells harboring the wild-type peptidine biosynthetic pathway. The node with the green hue represents pterin (4) networked into the untargeted wild-type map. This network includes abundant molecules from the pathway in addition to primary metabolites and media components.

DOI: [10.7554/eLife.25229.010](https://doi.org/10.7554/eLife.25229.010)

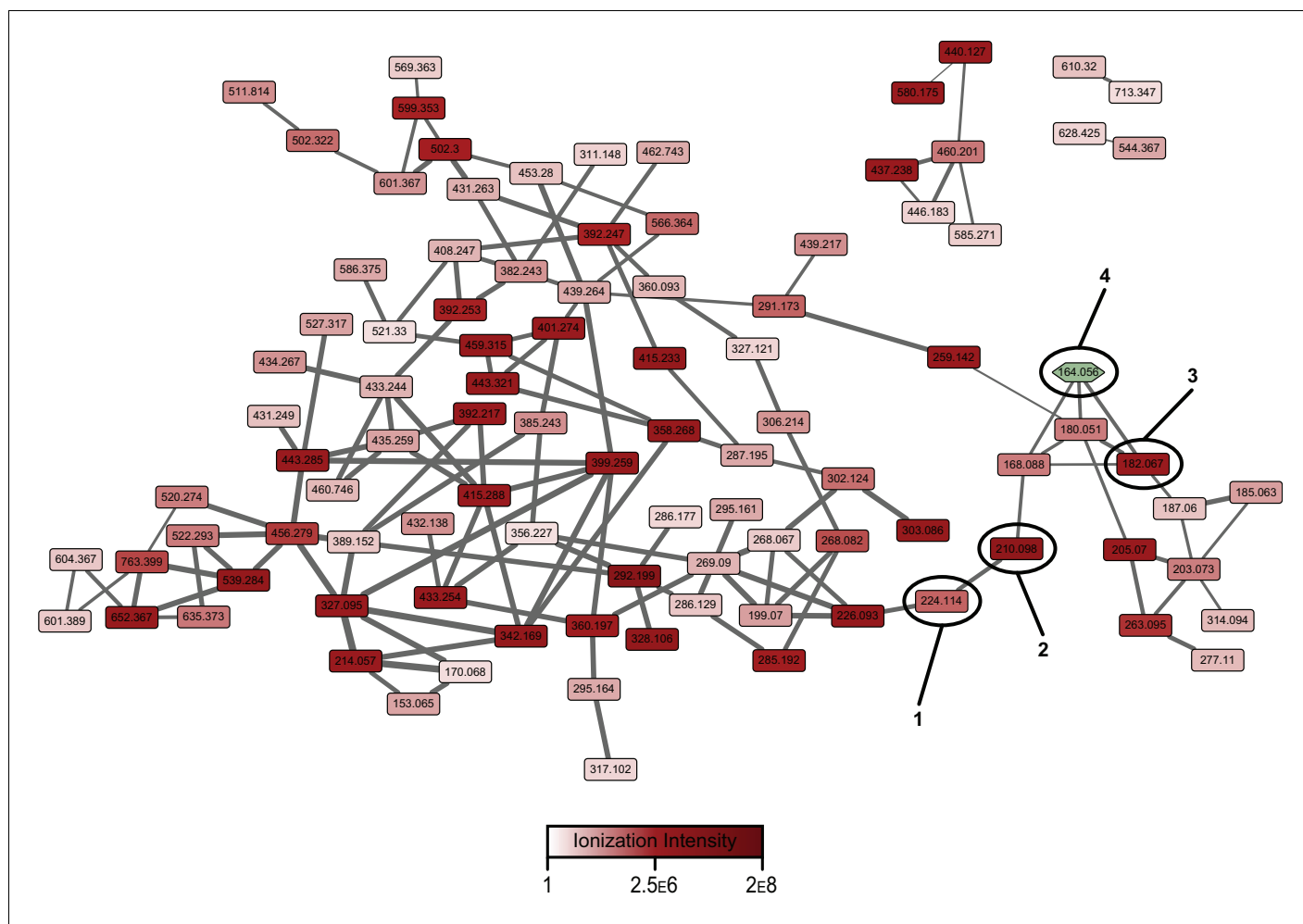


**Figure 3—figure supplement 2.** Pathway-targeted molecular networking of the wild-type peptidine biosynthetic pathway. Comparative metabolomic analysis between control and experimental culture samples enabled targeting ( $MS^2$ ) of molecular features dependent on the presence of the biosynthetic pathway.

DOI: [10.7554/eLife.25229.011](https://doi.org/10.7554/eLife.25229.011)

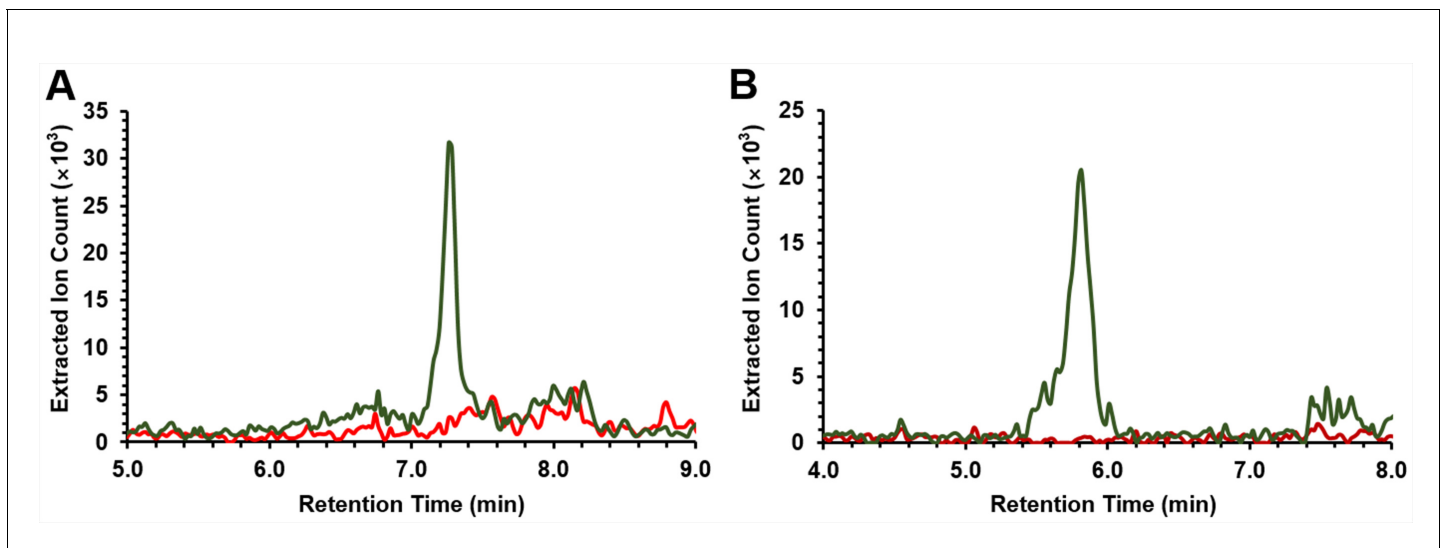


**Figure 3—figure supplement 3.** LC/MS Extracted Ion Count (EIC) chromatograms of compounds 1 (A) and 2 (B) from butanol extracts of the peptertidine heterologous expression strain. LC/MS traces were extracted with  $m/z$  224 corresponding to compound 1 (A) and  $m/z$  210 corresponding to compound 2 (B) from butanol extracts of the *E. coli* BAP1 culture broths carrying the wild-type peptertidine pathway (green) or the empty vector (pET28a, red).

DOI: [10.7554/eLife.25229.012](https://doi.org/10.7554/eLife.25229.012)

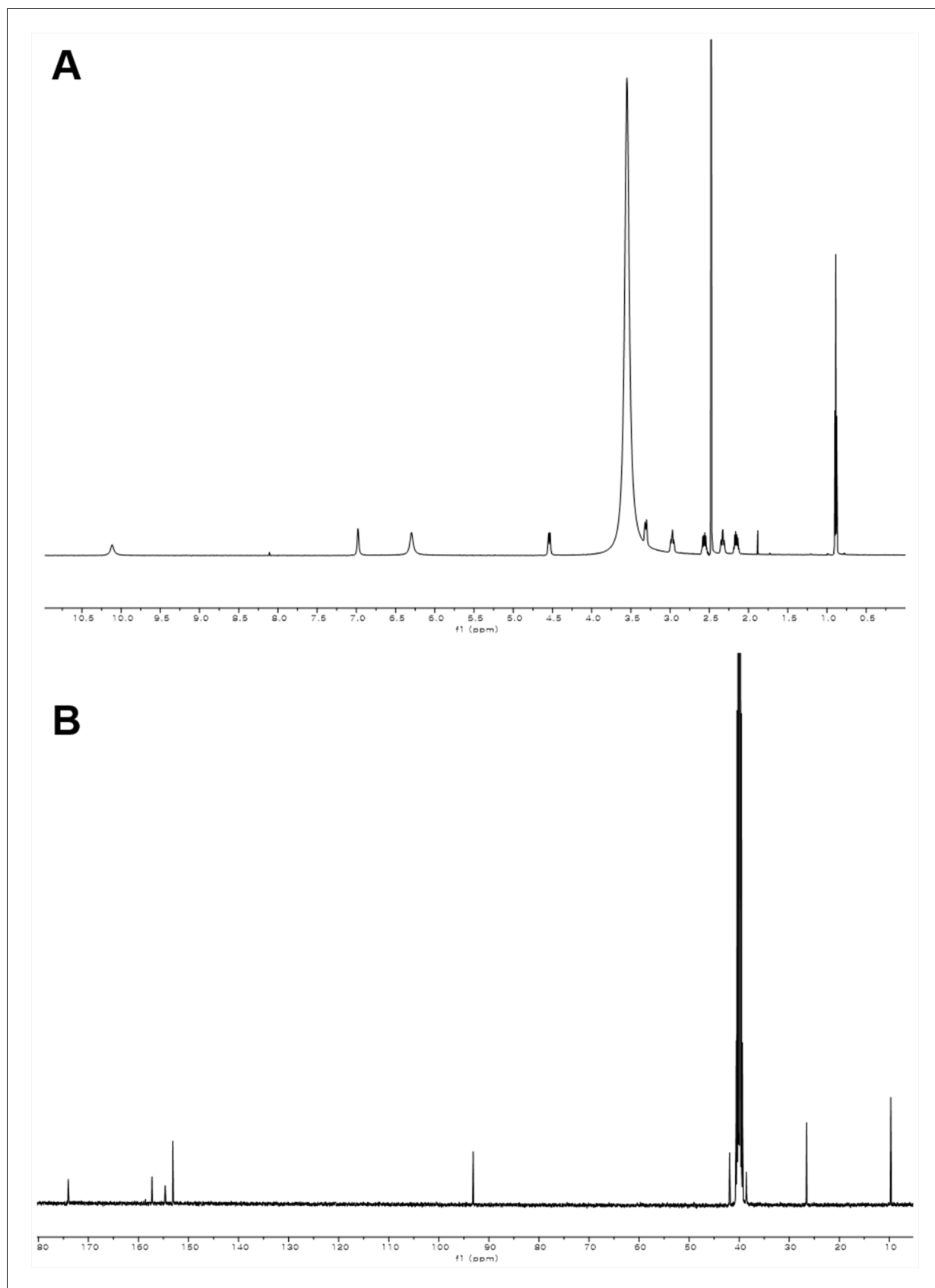


**Figure 3—figure supplement 4.**  $^1\text{H}$  and  $^{13}\text{C}$  NMR spectra of compound 1. (A)  $^1\text{H}$  NMR spectrum of compound 1 in DMSO- $d_6$ . (B)  $^{13}\text{C}$  NMR spectrum of compound 1 in DMSO- $d_6$ .

DOI: [10.7554/eLife.25229.013](https://doi.org/10.7554/eLife.25229.013)

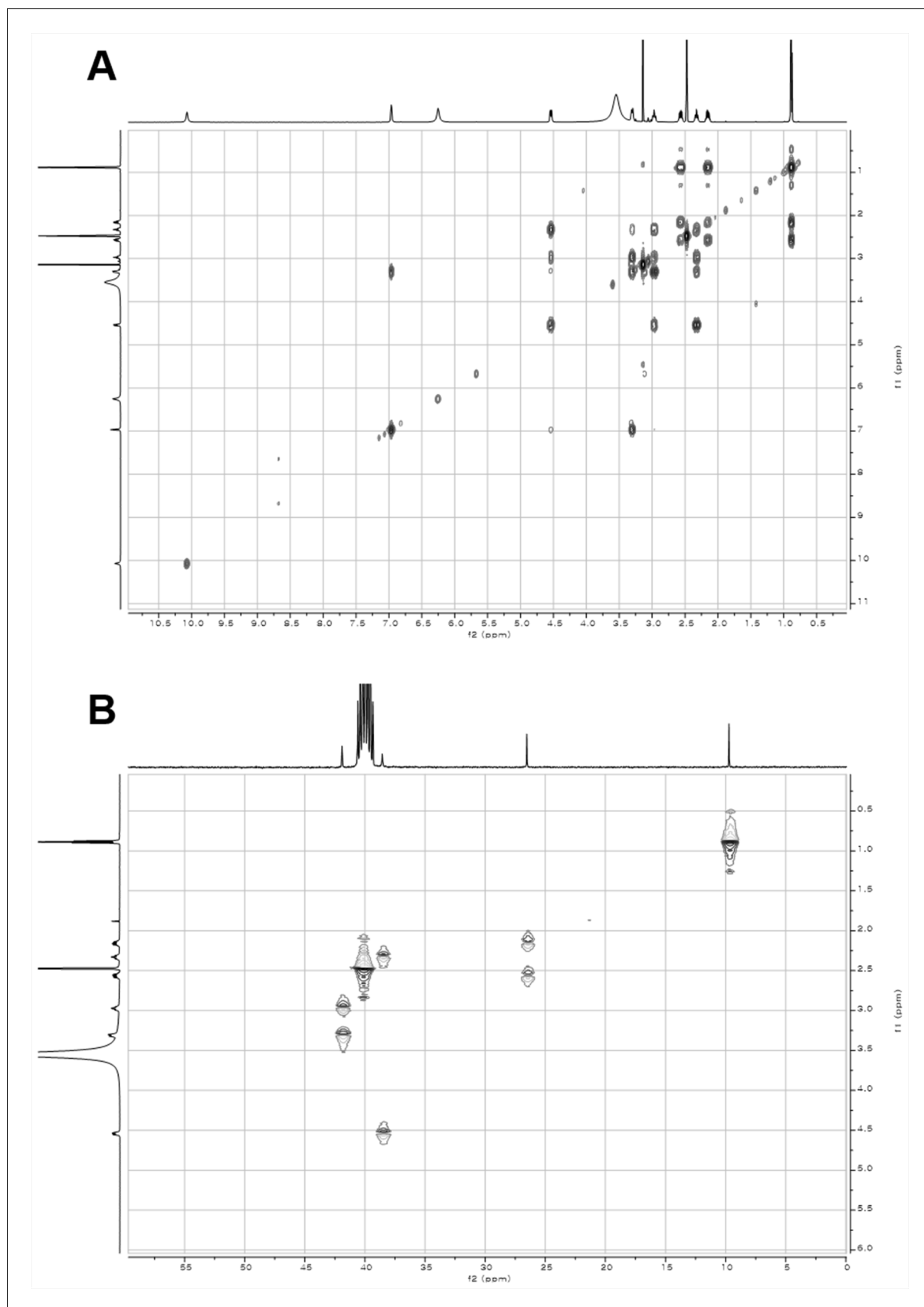


**Figure 3—figure supplement 5.** 2D- (gCOSY and gHSQCAD) NMR spectra of compound **1**. (A) gCOSY NMR spectrum of compound **1** in DMSO- $d_6$ . (B) gHSQCAD NMR spectrum of compound **1** in DMSO- $d_6$ .

DOI: [10.7554/eLife.25229.014](https://doi.org/10.7554/eLife.25229.014)



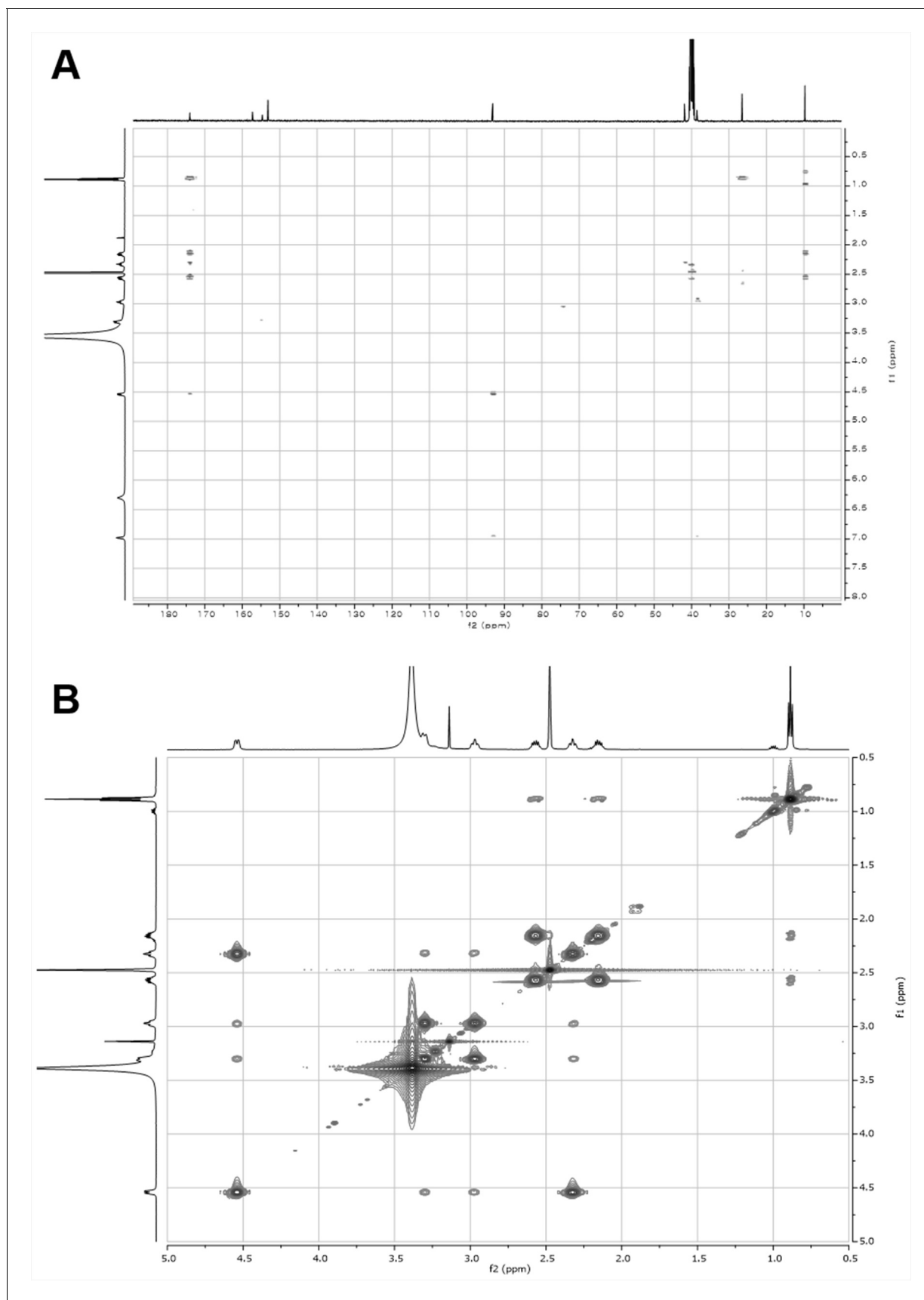


**Figure 3—figure supplement 6.** 2D- (gHMBCAD and NOESY) NMR spectra of compound **1**. (A) gHMBCAD NMR spectrum of compound **1** in DMSO- $d_6$ . (B) NOESY NMR spectrum of compound **1** in DMSO- $d_6$ .

DOI: [10.7554/eLife.25229.015](https://doi.org/10.7554/eLife.25229.015)

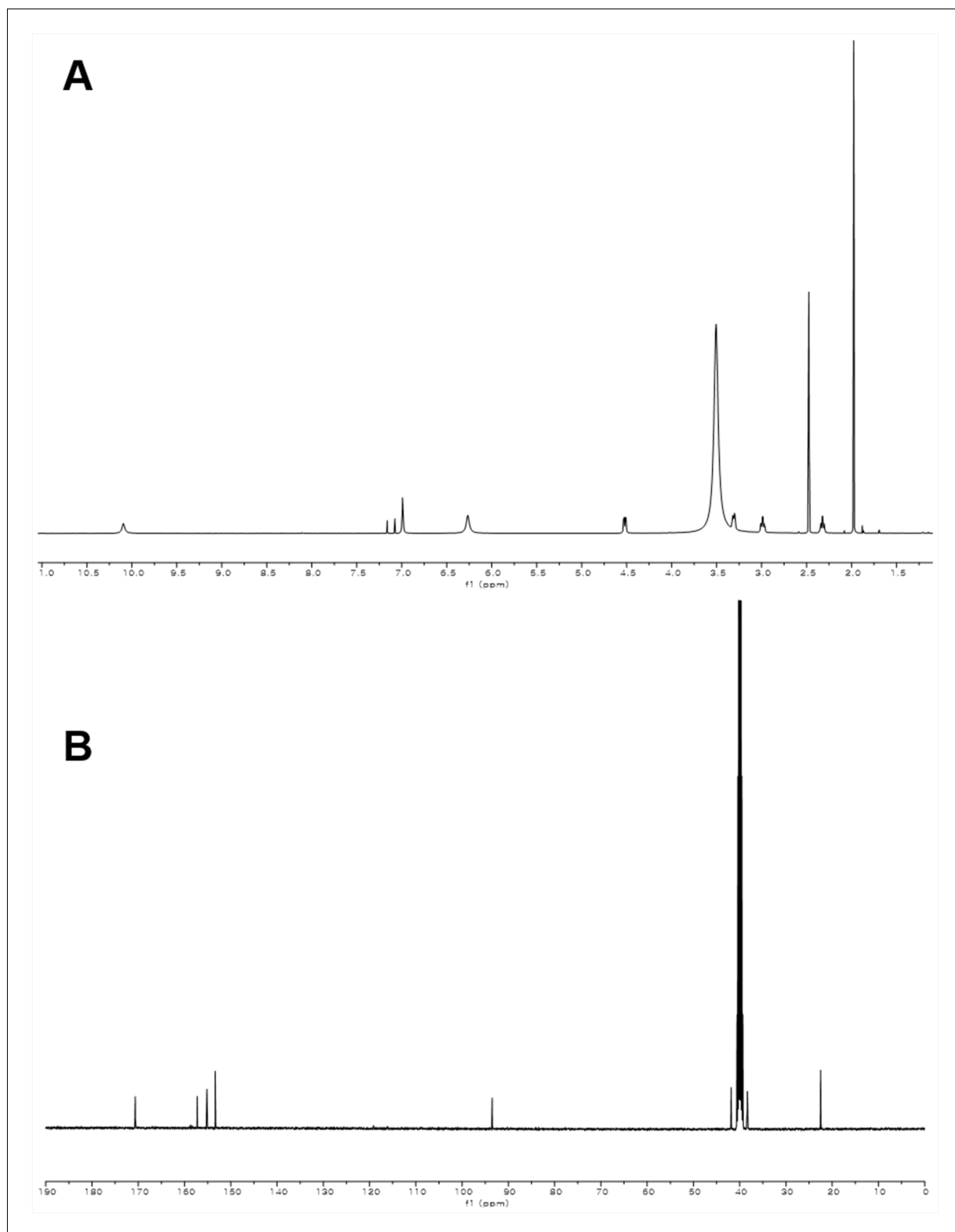


**Figure 3—figure supplement 7.**  $^1\text{H}$  and  $^{13}\text{C}$  NMR spectra of compound 2. (A)  $^1\text{H}$  NMR spectrum of compound 2 in DMSO- $d_6$ . (B)  $^{13}\text{C}$  NMR spectrum of compound 2 in DMSO- $d_6$ .

DOI: [10.7554/eLife.25229.016](https://doi.org/10.7554/eLife.25229.016)

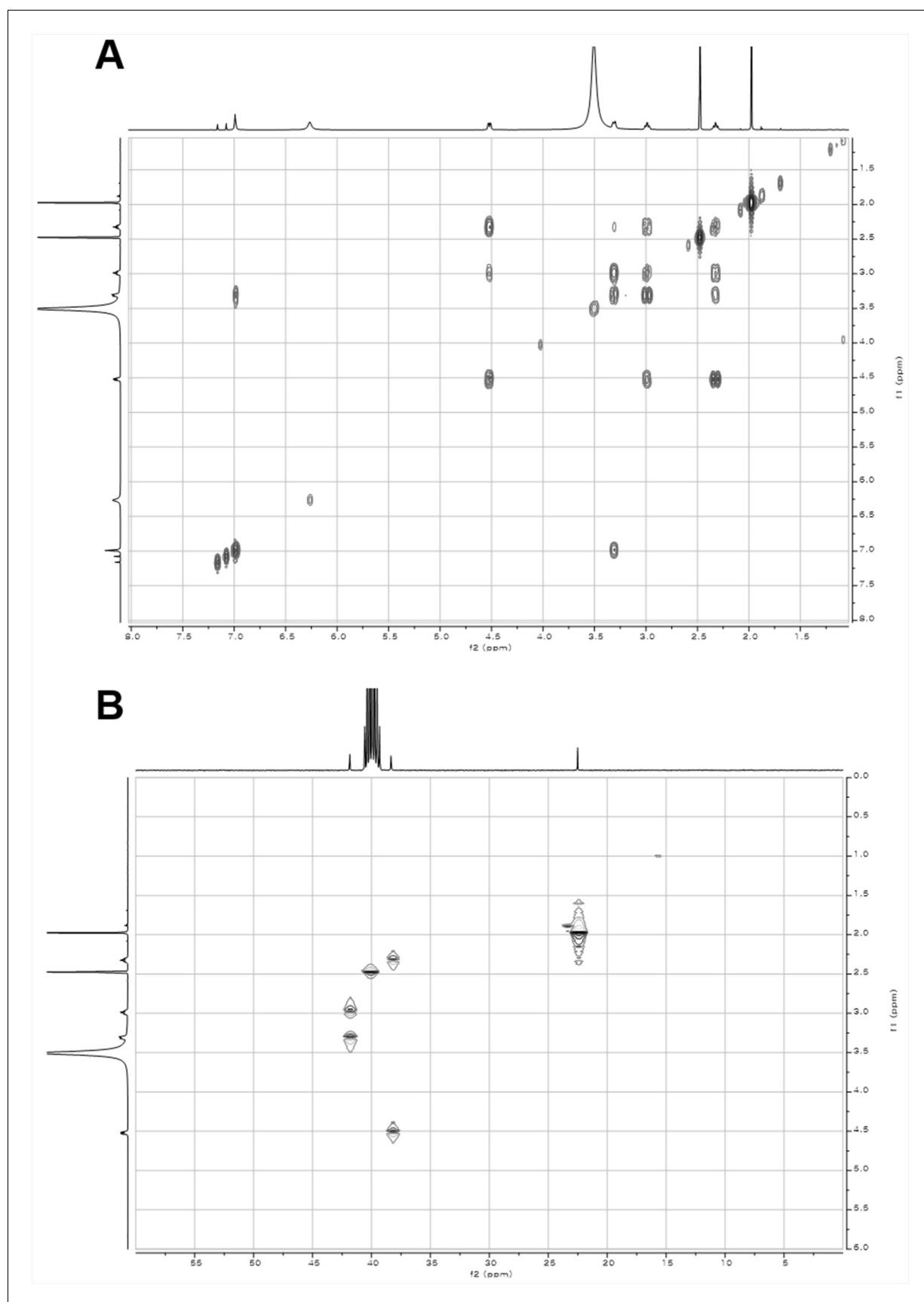


**Figure 3—figure supplement 8.** 2D- (gCOSY and gHSQCAD) NMR spectra of compound **2**. (A) gCOSY NMR spectrum of compound **2** in DMSO- $d_6$ . (B) gHSQCAD NMR spectrum of compound **2** in DMSO- $d_6$ .

DOI: [10.7554/eLife.25229.017](https://doi.org/10.7554/eLife.25229.017)

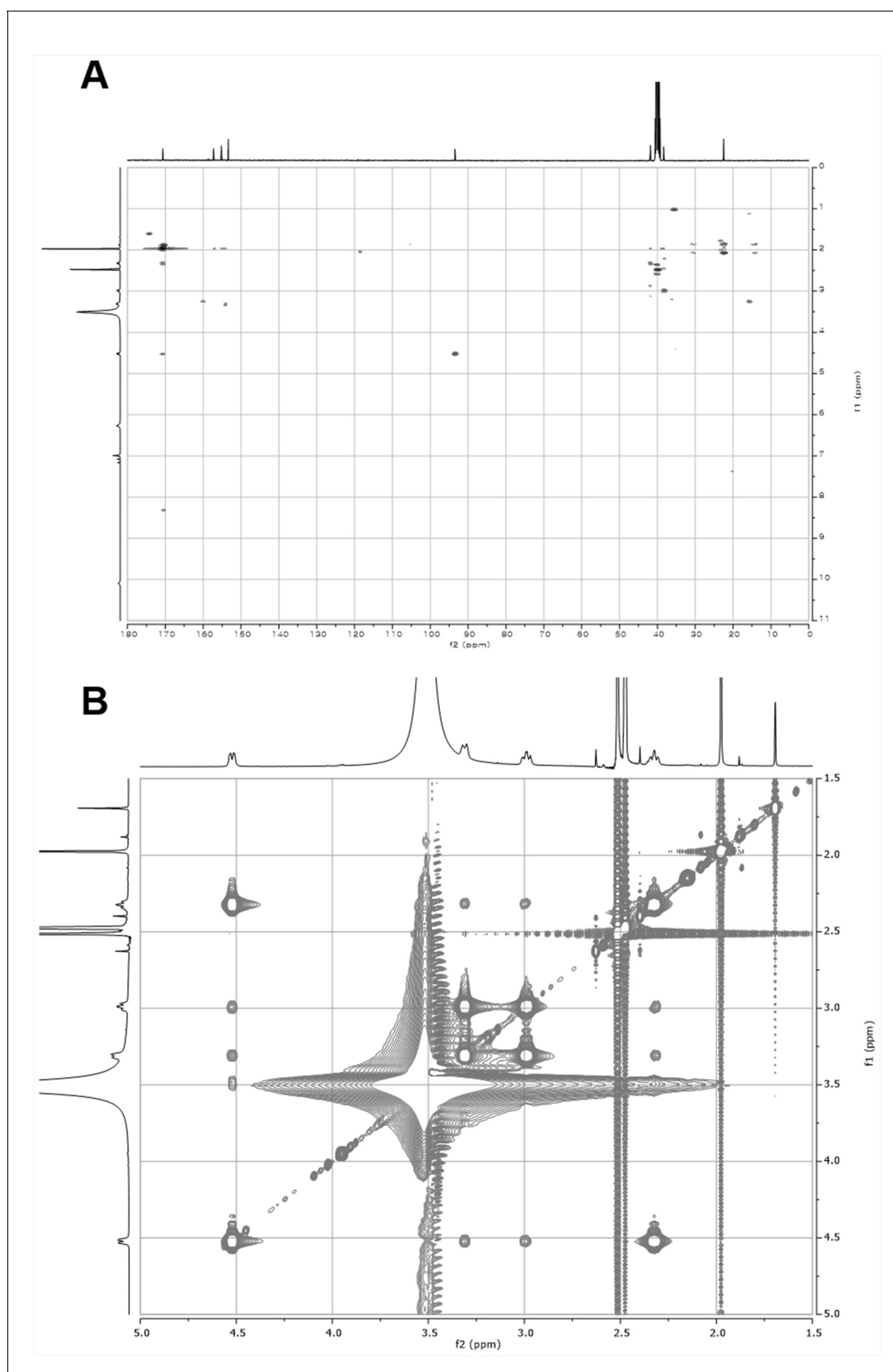


**Figure 3—figure supplement 9.** 2D- (gHMBCAD and NOESY) NMR spectra of compound 2. (A) gHMBCAD NMR spectrum of compound 2 in DMSO- $d_6$ . (B) NOESY NMR spectrum of compound 2 in DMSO- $d_6$ .

Figure 3—figure supplement 9 continued on next page

Figure 3—figure supplement 9 continued

DOI: [10.7554/eLife.25229.018](https://doi.org/10.7554/eLife.25229.018)

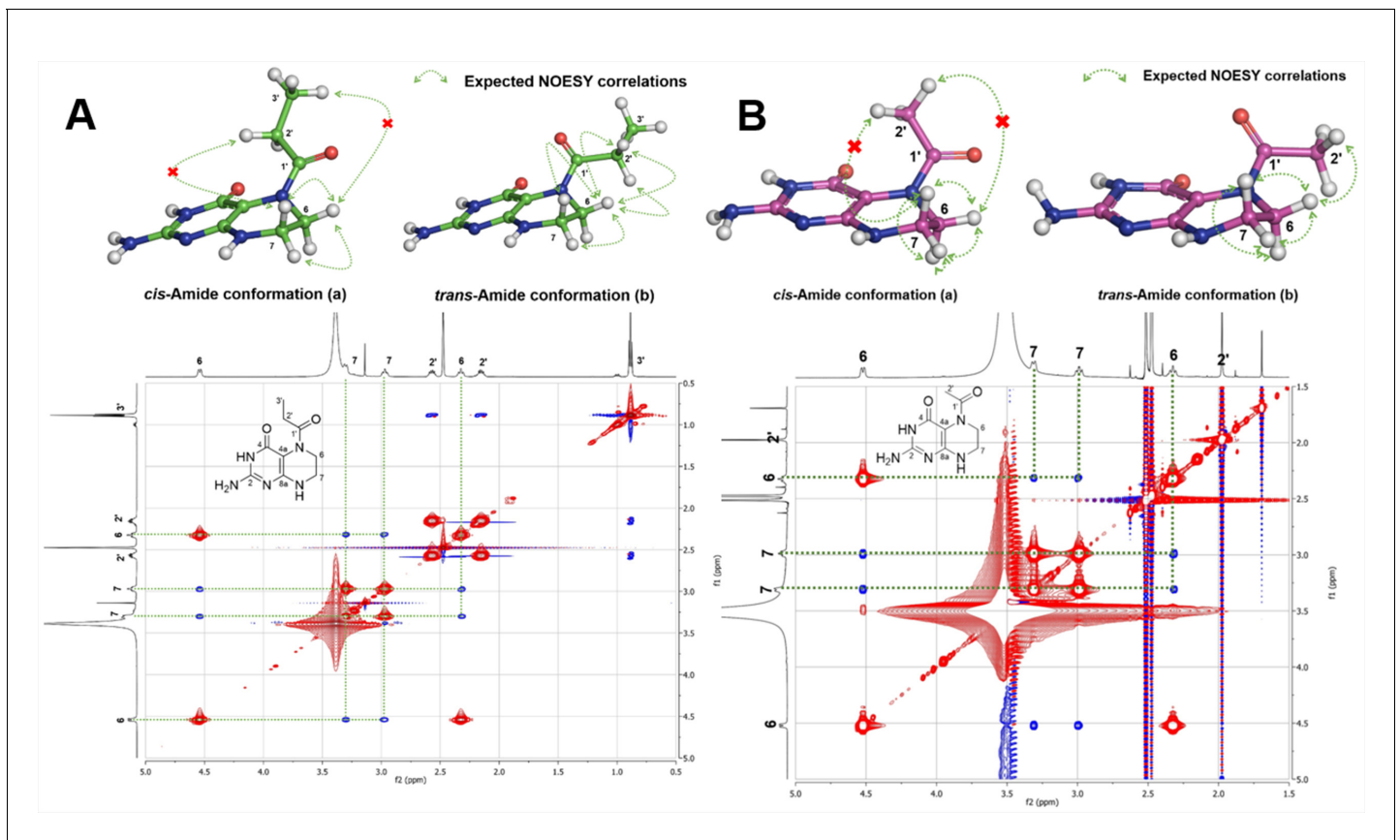


**Figure 3—figure supplement 10.** Amide conformation of compounds 1 and 2. (A) Plausible *cis*- (a) and *trans*- (b) amide conformations of compound 1 (top) and interpretation of 2D NOESY spectral data of compound 1 (bottom), (B) Plausible *cis*- (a) and *trans*- (b) amide conformations of compound 2 (top) and interpretation of 2D NOESY spectral data of compound 2 (bottom).

DOI: [10.7554/eLife.25229.019](https://doi.org/10.7554/eLife.25229.019)



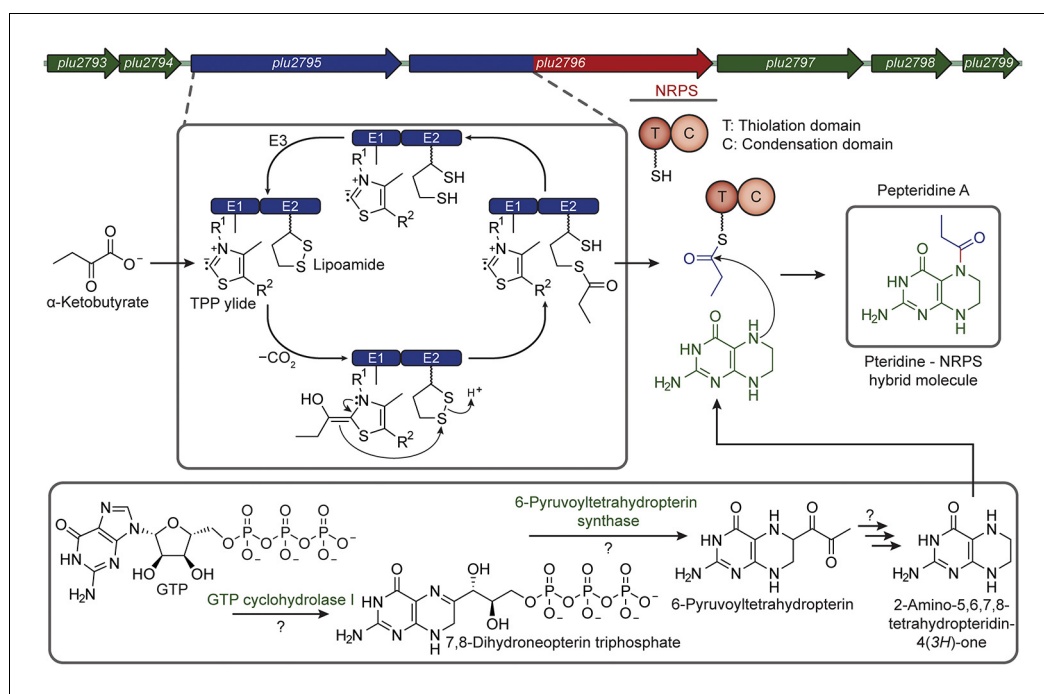


**Figure 4.** Proposed peptidine biosynthesis.  $\alpha$ -Ketobutyrate is processed by the atypical dehydrogenase-NRPS-like complex to generate a propionyl-loaded carrier protein (blue). Pteridine enzymes interact with the metabolism of the host to generate tetrahydropterin (green). The NRPS C domain couples these substrates to form the *cis*-amide bond (red) as illustrated for 1.

DOI: [10.7554/eLife.25229.021](https://doi.org/10.7554/eLife.25229.021)

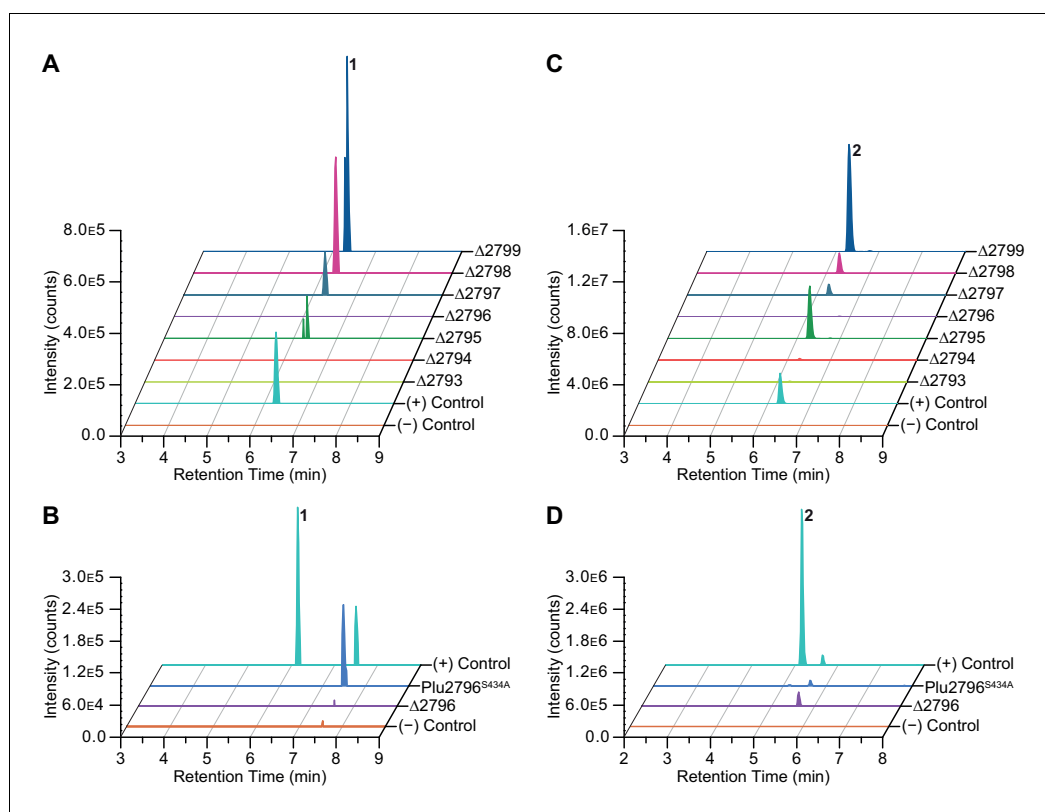


**Figure 5.** Gene deletion and NRPS inactivation analyses on 1 (A–B) and 2 (C–D). (A–B) Extracted ion chromatograms of 1 for wild-type and mutants are shown. (C–D) Extracted ion chromatograms of 2 for wild-type and mutants are shown.

DOI: [10.7554/eLife.25229.022](https://doi.org/10.7554/eLife.25229.022)

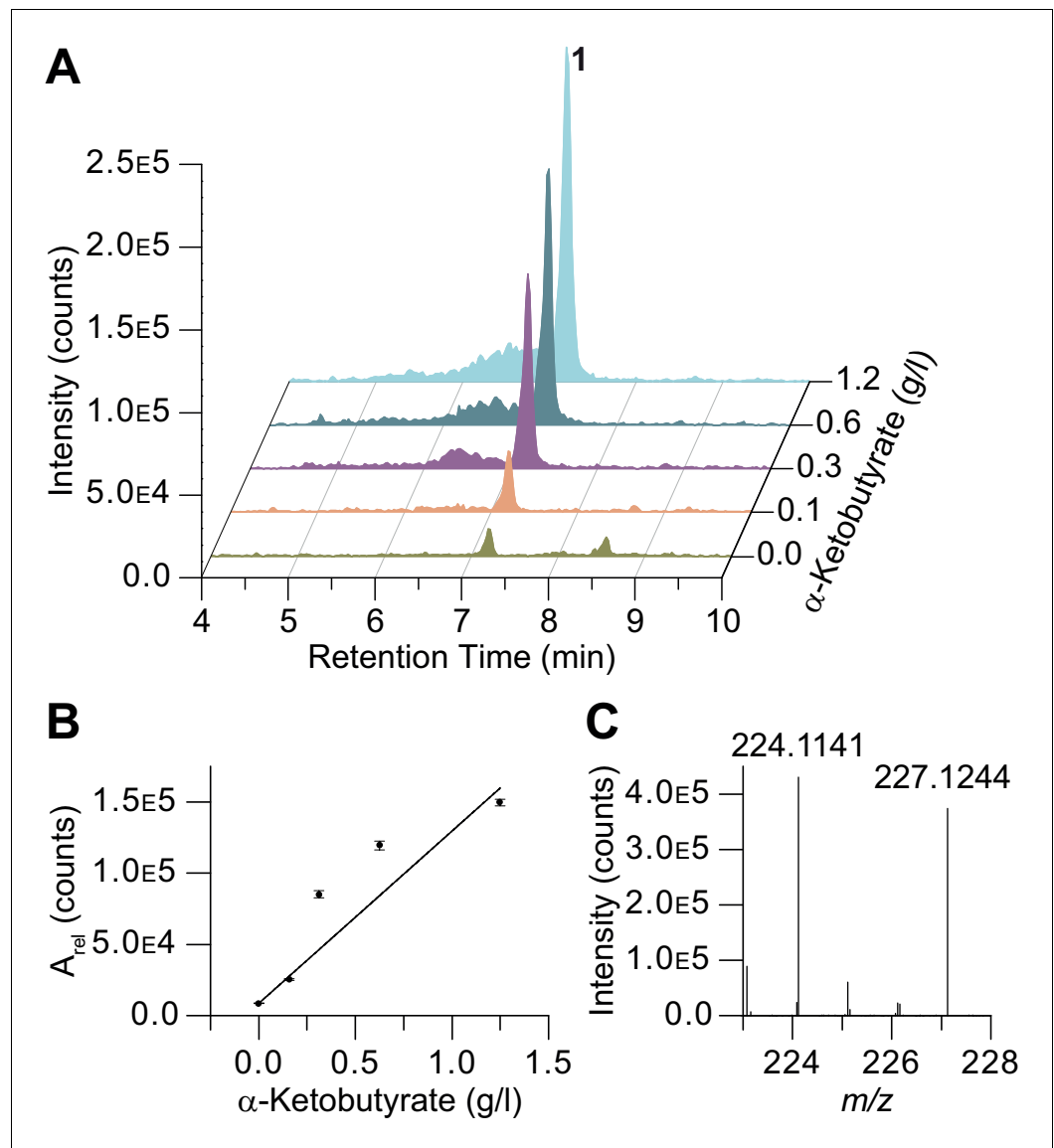


**Figure 6.**  $\alpha$ -Ketobutyrate feeding studies on 1. (A–B) Production enhancement of 1 in  $\alpha$ -ketobutyrate supplementation studies ( $A_{rel}$ , relative integration value). (C)  $^{13}\text{C}_4$ - $\alpha$ -ketobutyrate supplementation leads to  $^{13}\text{C}_3$  incorporation in 1 consistent with the proposed biosynthesis.

DOI: [10.7554/eLife.25229.023](https://doi.org/10.7554/eLife.25229.023)

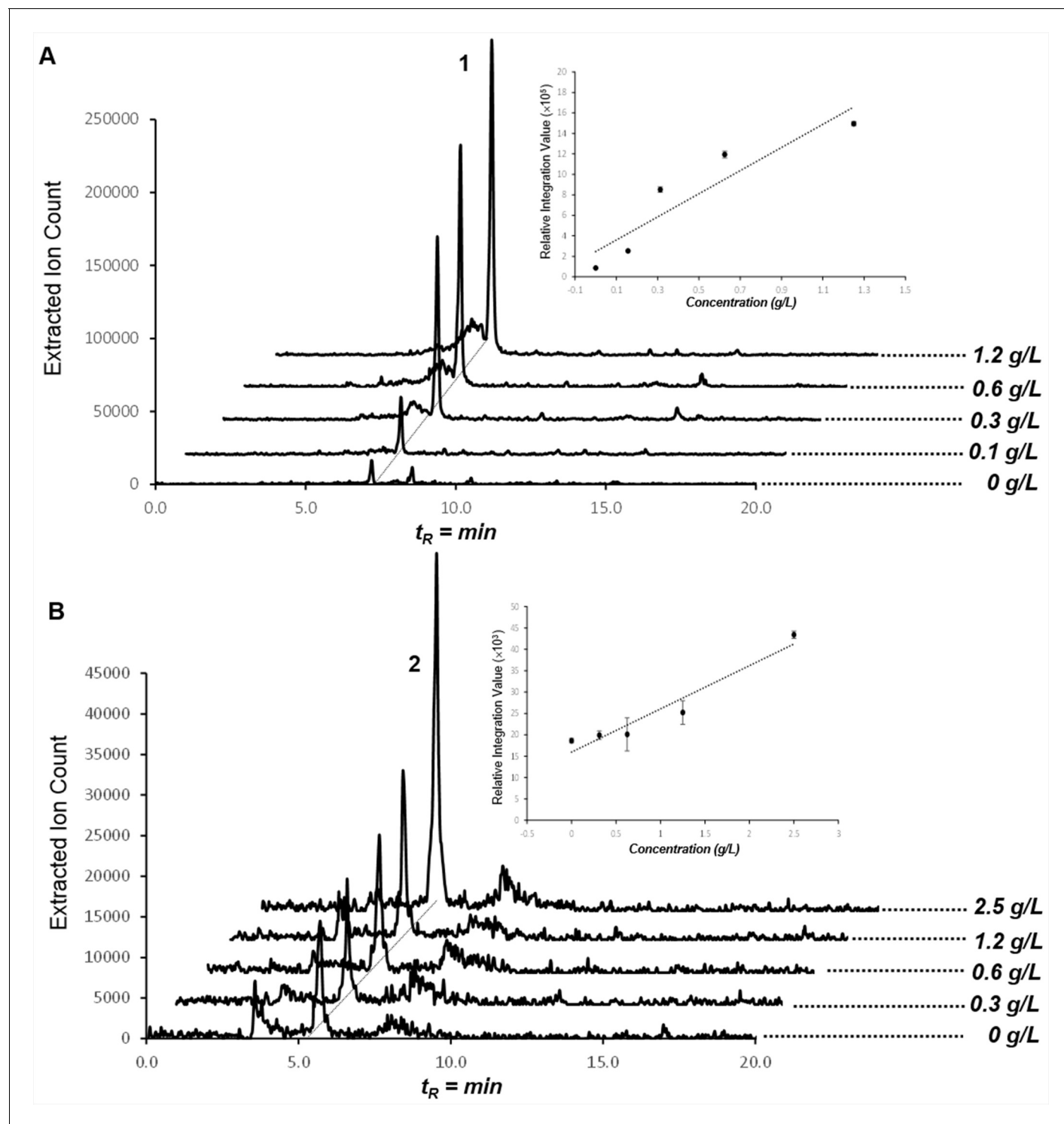


**Figure 6—figure supplement 1.** Production of compounds 1 and 2 in dose-dependent  $\alpha$ -ketobutyrate (A) and pyruvate (B) feeding studies. HPLC/MS traces were extracted with  $m/z$  224 corresponding to compound 1 (A) and  $m/z$  210 corresponding to compound 2 (B) from butanol extracts of the culture broths fed with varying concentrations of  $\alpha$ -ketobutyrate (A) and pyruvate (B). Dose-response plots for 1 and 2 were determined using extracted peak integration values.

DOI: [10.7554/eLife.25229.024](https://doi.org/10.7554/eLife.25229.024)

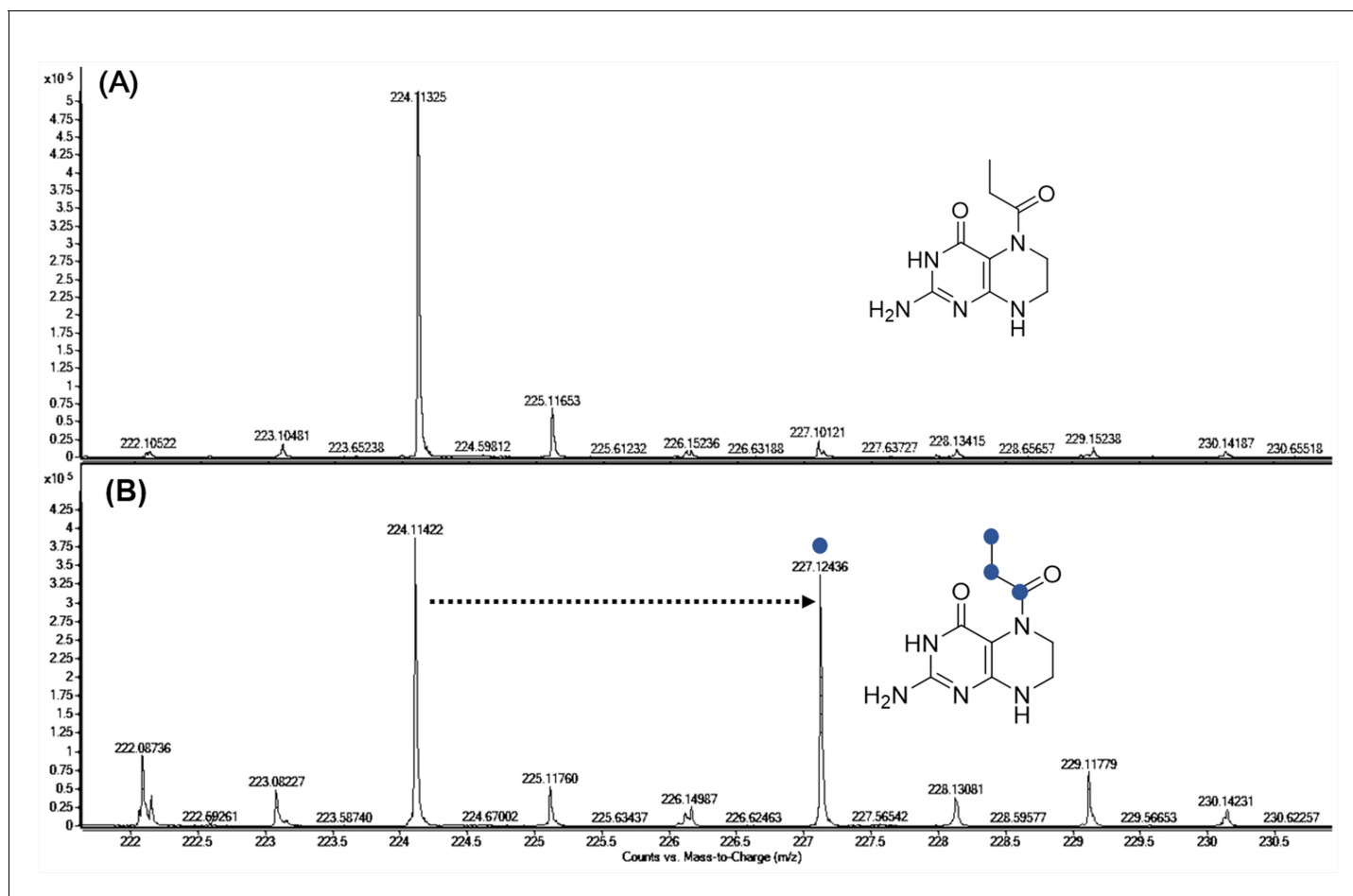


**Figure 6—figure supplement 2.** Characterization of  $^{13}\text{C}_4$ - $\alpha$ -ketobutyrate incorporation in compound 1. Incorporation of  $^{13}\text{C}_4$ - $\alpha$ -ketobutyrate into compound 1 (B) led to a clear 3 Da mass shift of native 1 (A) via oxidative decarboxylation of  $\alpha$ -ketobutyrate.

DOI: [10.7554/eLife.25229.025](https://doi.org/10.7554/eLife.25229.025)

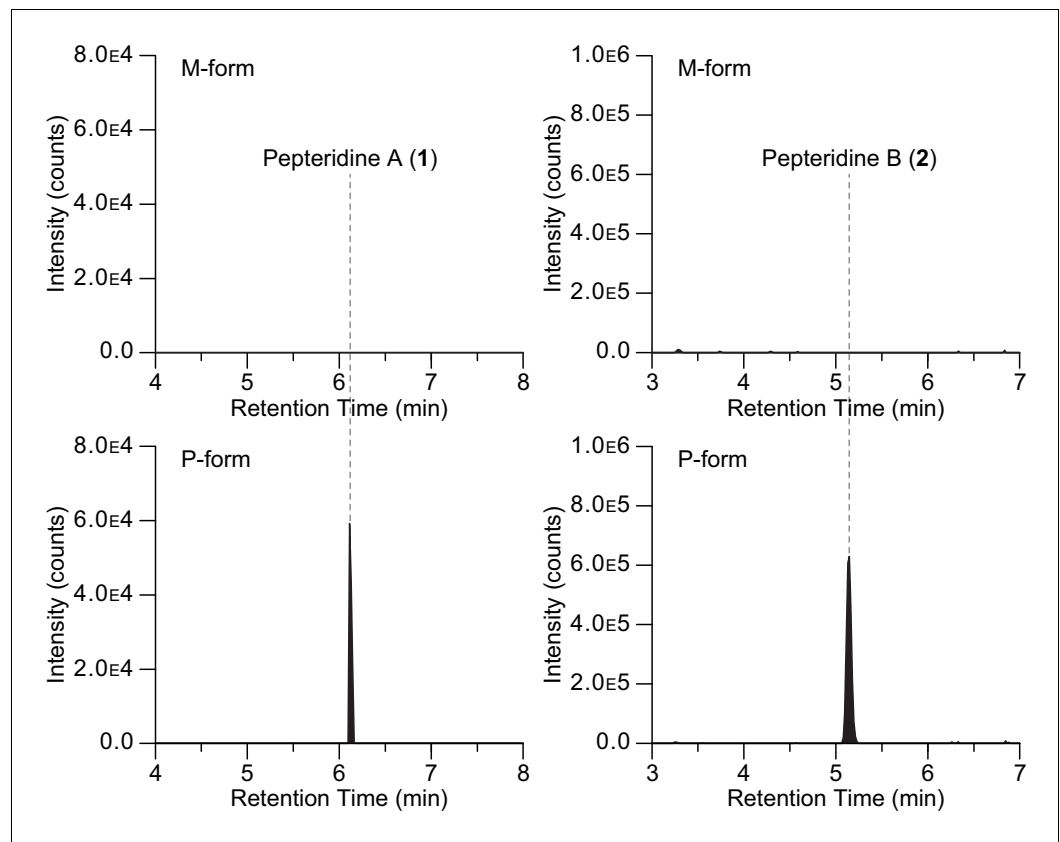


**Figure 7.** Extracted ion counts LC/HR-ESI-QTOF-MS analysis of peptRIDines A (left panel) and B (right panel) from two genetically engineered *P. luminescens* strains locked in the phenotypic variants M-form (top) and P-form (bottom).

DOI: [10.7554/eLife.25229.026](https://doi.org/10.7554/eLife.25229.026)

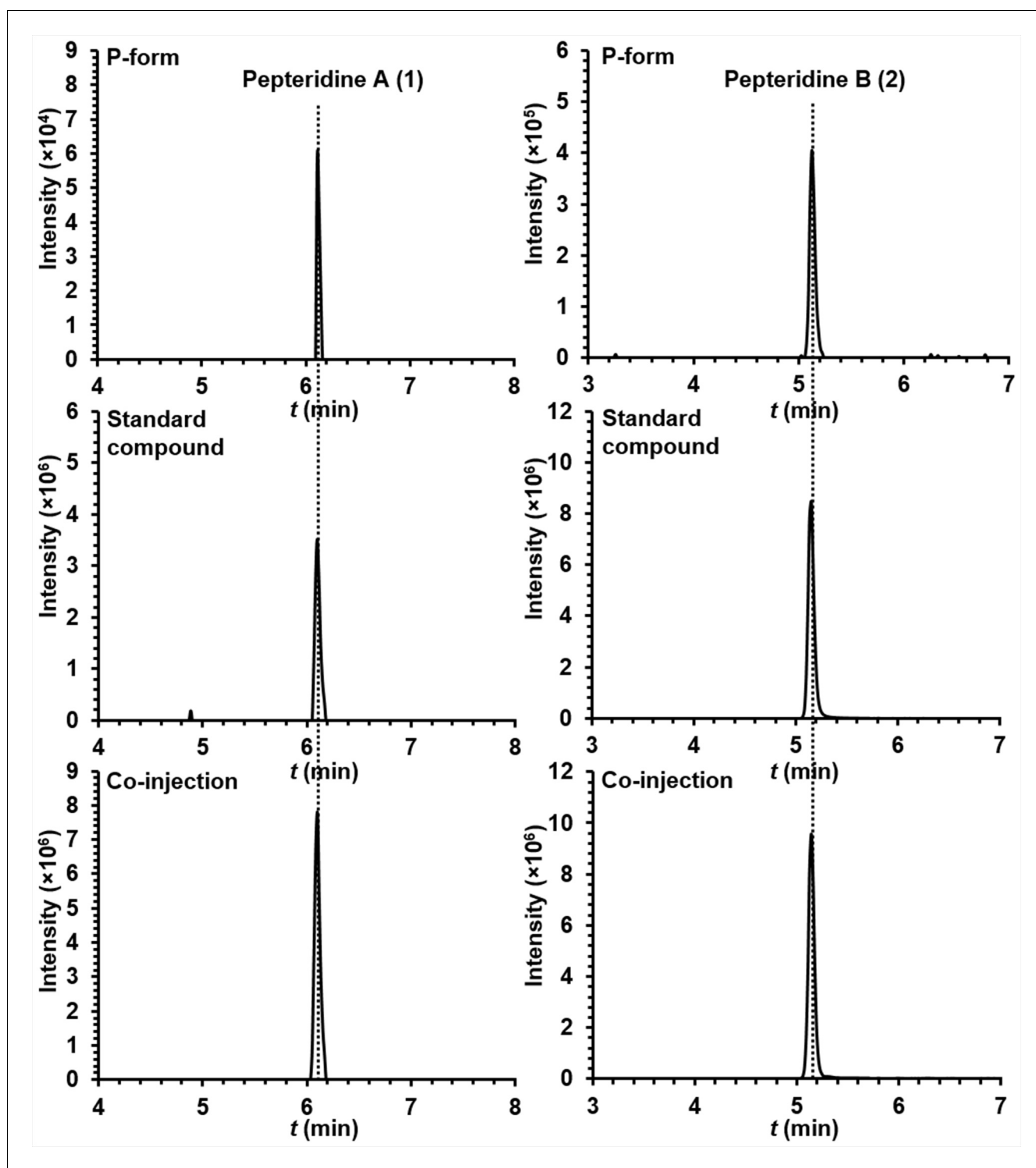


**Figure 7—figure supplement 1.** Extracted ion counts chromatograms from LC/HR-ESI-QTOF-MS analysis of pepteridines A (left panel) and B (right panel) from the butanol extracts of P-form culture broth (top), standard compounds (middle), and co-injection (bottom).

DOI: [10.7554/eLife.25229.027](https://doi.org/10.7554/eLife.25229.027)

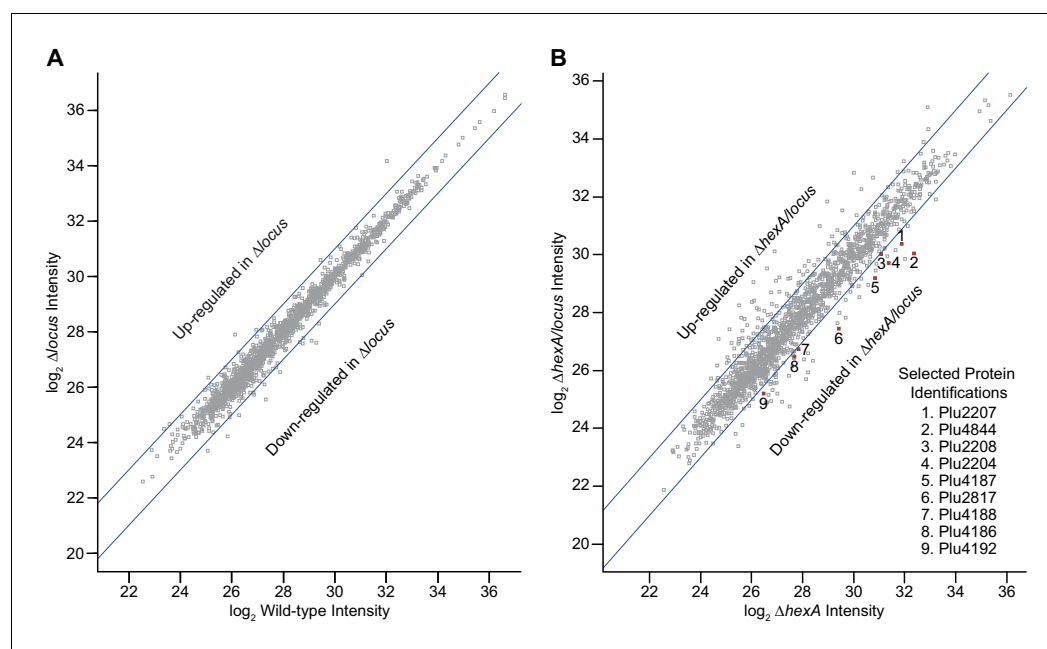


**Figure 8.** Quantitative proteomic analysis of a  $\Delta$ locus strain in a wild-type background (A) and  $\Delta$ hexA background (B).

DOI: [10.7554/eLife.25229.028](https://doi.org/10.7554/eLife.25229.028)

The following source data is available for figure 8:

**Source data 1.** Proteins increased in WT vs. WT $\Delta$ locus strains by LC-MS/MS.

DOI: [10.7554/eLife.25229.029](https://doi.org/10.7554/eLife.25229.029)

**Source data 2.** Proteins increased in WT $\Delta$ locus vs. WT strains by LC-MS/MS.

DOI: [10.7554/eLife.25229.030](https://doi.org/10.7554/eLife.25229.030)

**Source data 3.** Proteins increased in  $\Delta$ hexA vs.  $\Delta$ hexA $\Delta$ locus strains by LC-MS/MS.

DOI: [10.7554/eLife.25229.031](https://doi.org/10.7554/eLife.25229.031)

**Source data 4.** Proteins increased in  $\Delta$ hexA $\Delta$ locus vs.  $\Delta$ hexA strains by LC-MS/MS.

DOI: [10.7554/eLife.25229.032](https://doi.org/10.7554/eLife.25229.032)

**Source data 5.** All proteins observed in WT and WT $\Delta$ locus strains by LC-MS/MS.

DOI: [10.7554/eLife.25229.033](https://doi.org/10.7554/eLife.25229.033)

**Source data 6.** All proteins observed in  $\Delta$ hexA and  $\Delta$ hexA $\Delta$ locus strains by LC-MS/MS.

DOI: [10.7554/eLife.25229.034](https://doi.org/10.7554/eLife.25229.034)